

DMD17145

Glucuronidation of active tamoxifen metabolites by the human UDP-glucuronosyltransferases (UGTs)

Dongxiao Sun, Arun K. Sharma, Ryan Dellinger, Andrea S. Blevins-Primeau, Renee Balliet, Gang Chen, Telih Boyiri, Shantu Amin, and Philip Lazarus

Cancer Prevention and Control (D.S., R.D., A.S.B-P., R.B., G.C. P.L.) and Chemical Carcinogenesis and Chemoprevention (A.K.S., T.B., S.A.) Programs, Penn State Cancer Institute, Departments of Pharmacology (D.S., A.K.S., R.D., A.S.B-P., R.B., S.A., P.L.), Biochemistry and Molecular Biology (T.B.) and Public Health Sciences (G.C., P.L.), Penn State University College of Medicine, Hershey, PA 17033

DMD17145

Running title: Glucuronidation of tamoxifen metabolites

Corresponding author: Philip Lazarus, Ph.D., Penn State Cancer Institute, Penn State University College of Medicine, Rm. C3739D, MC-H069, 500 University Drive, Hershey, PA 17033. Tel: (717)-531-5734; Fax: (717) 531-0480; Email: plazarus@psu.edu

Number of text pages: 36

Number of Tables: 2

Number of Figures: 5

References: 39

Number of words in Abstract: 249;

Number of words in Introduction: 724;

Number of words in Discussion: 724.

Abbreviations: TAM, tamoxifen; 4-OH-TAM, 4-hydroxytamoxifen; endoxifen, 4-hydroxy-N-desmethyl-tamoxifen; UGT, UDP-glucuronosyltransferase; UDPGA, UDP-glucuronic acid; DMEM, Dulbecco's modified Eagles medium; FBS, fetal bovine serum; NMR, nuclear magnetic resonance; HPLC, high pressure liquid chromatography; LC-MS, liquid chromatography-mass spectrometry; HLMS, human liver microsomes; K_M , Michaelis-Menten equilibrium constant; V_{max} , maximal velocity.

DMD17145

Abstract

Tamoxifen (TAM) is an anti-estrogen that has been widely used in the treatment and prevention of breast cancer in women. One of the major mechanisms of metabolism and elimination of TAM and its major active metabolites, 4-hydroxy (OH)-TAM and 4-OH-N-desmethyl-TAM (endoxifen), is via glucuronidation. While limited studies have been performed characterizing the glucuronidation of 4-OH-TAM, no studies have been performed on endoxifen. In the present study, characterization of the glucuronidating activities of human UGTs against isomers of 4-OH-TAM and endoxifen was performed. Using homogenates of individual UGT-overexpressing cell lines, UGTs 2B7 \approx 1A8 > UGT1A10 exhibited the highest overall O-glucuronidating activity against *trans*-4-OH-TAM as determined by V_{\max}/K_M , with the hepatic enzyme, UGT2B7, exhibiting the highest binding affinity and lowest K_M (3.7 μ M). As determined by V_{\max}/K_M , UGT1A10 exhibited the highest overall O-glucuronidating activity against *cis*-4-OH-TAM, 10-fold higher than the next-most active UGTs 1A1 and 2B7, but with UGT1A7 exhibiting the lowest K_M . While both *N*- and O-glucuronidation occurred for 4-OH-TAM in human liver microsomes, only O-glucuronidating activity was observed for endoxifen; no endoxifen-*N*-glucuronidation was observed for any UGT tested. UGTs 1A10 \approx 1A8 > UGT2B7 exhibited the highest overall glucuronidating activities as determined by V_{\max}/K_M for *trans*-endoxifen, with the extra-hepatic enzyme, UGT1A10, exhibiting the highest binding affinity and lowest K_M (39.9 μ M). Similar to that observed for *cis*-4-OH-TAM, UGT1A10 also exhibited the highest activity for *cis*-endoxifen. These data suggest

DMD17145

that several UGTs including UGTs 1A10, 2B7 and 1A8 play an important role in the metabolism of 4-OH-TAM and endoxifen.

DMD17145

Introduction

TAM (1-[4-(2-dimethylaminoethoxy)-phenyl]-1,2-diphenylbut-1(Z)-ene) is a non-steroidal anti-estrogen that has been commonly used for the treatment and prevention of estrogen-dependent breast cancer (Fisher et al., 1998; Osborne, 1998; Cuzick et al., 2003; Howell et al., 2003). Adjuvant TAM treatment increases recurrence-free survival and overall survival in breast cancer patients with hormone receptor-positive tumors irrespective of their nodal status, menopausal status or age (Chowdhury and Ellis, 2005). In addition to its anti-estrogenic properties, which have been related to symptoms such as hot flashes, vaginal bleeding and pruritus vulvae (Osborne, 1998; Nechushtan and Peretz, 2002), TAM also has partial estrogen-agonistic effects that may be linked to reduced risk for ischemic heart disease and osteoporosis (McDonald and Stewart, 1991; Rutqvist and Mattsson, 1993), but may also increase the risk for endometrial cancer (van Leeuwen et al., 1994) and venous thromboembolism (Meier and Jick, 1998). Although TAM is generally well-tolerated, there is significant inter-individual variability in the clinical efficacy as well as toxicities of TAM. For instance, about 30% of patients acquire TAM resistance and relapse (1998). In addition, the relative risk of endometrial cancers in patients treated with TAM is estimated to be two- to three-fold that of controls, with risk increasing with both the duration and cumulative dose of TAM treatment (Fisher et al., 1994; Bergman et al., 2000). The mechanisms underlying variability in response to TAM and to TAM-related toxicities remains obscure. Since there is compelling evidence that TAM is converted to anti-estrogenic metabolites that are more potent than TAM itself, one hypothesis is that altered patterns of

DMD17145

metabolism of TAM and/or its primary metabolites might contribute to this inter-individual variability.

TAM is activated predominantly via cytochrome P450 (CYP450)-mediated pathways into several metabolites after oral administration, including the hydroxylated TAM metabolites, 4-OH-TAM and 4-hydroxy-*N*-desmethylTAM (endoxifen). Since both *trans*-4-OH-TAM and endoxifen exhibit up to 100-fold the levels of anti-estrogenic activity as compared to TAM and other TAM metabolites (Jordan et al., 1977; Lim et al., 2005), it is thought that they may be the major contributors to TAM's anti-estrogenic properties. While *cis*-4-OH-TAM is thought to possess some estrogen agonist activity, this isomer exhibits significant anti-estrogenic activity *in vitro* when in the presence of estradiol (Robertson et al., 1982; Murphy et al., 1990).

An important route of elimination and detoxification of TAM and its metabolites is via glucuronidation. TAM is excreted predominantly through the bile, a process largely facilitated by TAM conjugation to glucuronic acid during the glucuronidation process (Lien et al., 1989), and TAM glucuronides have been identified in the urine of TAM-treated patients (Poon et al., 1993). Most of the 4-OH-TAM found in the bile of TAM-treated patients was as a glucuronide conjugate (Lien et al., 1989). The fact that TAM metabolites are found in their unconjugated form in feces is likely due to β -glucuronidase-catalyzed de-glucuronidation within the microflora that colonize within the small intestine (Lien et al., 1989). TAM glucuronide conjugates have been identified in the serum of TAM-treated patients (Lien et al., 1989), and it has been suggested that glucuronidation within target tissues like the adipose tissue of the breast may also be important in terms of TAM metabolism and overall TAM activity (Nowell et al., 2005).

DMD17145

Microsomes from human liver specimens exhibit high glucuronidating activities toward TAM to form TAM-*N*⁺-glucuronide and both the *trans* and *cis* isomers of 4-OH-TAM to form 4-OH-TAM-*N*⁺- and 4-OH-TAM-O-glucuronides (Sun et al., 2006). One of the UGTs involved in the glucuronidation of TAM and its metabolites is the hepatic enzyme, UGT1A4 (Nishiyama et al., 2002; Kaku et al., 2004), which catalyzes the formation of a quarternary ammonium-linked glucuronide with TAM's or 4-OH-TAM's *N,N*-dimethylaminoalkyl side chain (Kaku et al., 2004). This pattern of ammonium-linked glucuronidation is consistent with UGT1A4's glucuronidation activity against primary, secondary and tertiary amines present in a variety of carcinogenic compounds, androgens, progestins and plant steroids (Wiener et al., 2004a). In a screening of selected UGT-overexpressing baculosomes, UGTs 1A1, 1A3, 1A4, 1A8, 1A9, 2B7 and 2B15 were shown to exhibit activity against 4-OH-TAM (Kaku et al., 2004). However, a comprehensive characterization and kinetic analysis of the glucuronidating enzymes responsible for O-glucuronidation of TAM metabolites have not yet been performed, with no studies having yet been performed analyzing endoxifen glucuronidation. The goal of the present study was to characterize the glucuronidation of the TAM metabolites, 4-OH-TAM and endoxifen, and identify the UGTs active in this pathway.

DMD17145

Materials and Methods

Chemicals and materials. *trans*-4-OH-TAM (98% pure), *trans*-4-OH-TAM/*cis*-4-OH-TAM mixture (70:30% ratio), UDPGA, alamethicin, β -glucuronidase, anti-calnexin antibody and bovine serum albumin were purchased from Sigma-Aldrich (St. Louis, MO). Ethylchloroformate, toluene, ethyleneglycol, hydrazine hydrate, diethyl ether were purchased from Aldrich Chemical Co. (Milwaukee, WI). Dulbecco's modified Eagles medium (DMEM), Dulbecco's phosphate-buffered saline (minus calcium-chloride and magnesium-chloride), fetal bovine serum (FBS), penicillin-streptomycin and geneticin (G418) were purchased from Gibco (Grand Island, NY). The Platinum® *Pfx* DNA polymerase and the pcDNA3.1/V5-His-TOPO mammalian expression vector were obtained from Invitrogen (Carlsbad, CA) while the restriction enzymes DpnI and StuI were purchased from New England Biolabs (Beverly, MA). The BCA protein assay kit was purchased from Pierce (Rockford, IL) while the QIAEX® II gel extraction kit was purchased from Qiagen (Valencia, CA). The human UGT1A and UGT2B7 Western blotting kits and the anti-UGT1A and anti-UGT2B7 antibodies were purchased from Gentest (Woburn, MA). All other chemicals used were purchased from Fisher Scientific (Pittsburgh, PA) unless otherwise specified.

Tissues and cell lines. A description of the normal human liver tissue specimens used for these studies was described previously (Wiener et al., 2004b). Briefly, tissues were quick-frozen at -70°C within 2 hours post-surgery. Liver microsomes were prepared through differential centrifugation as previously described (Coughtrie et al., 1986) and were stored (10-20 mg protein/ml) at -80°C . Microsomal

DMD17145

protein concentrations were measured using the BCA assay. All protocols involving the analysis of tissue specimens were approved by the institutional review board at the Penn State College of Medicine and in accordance with assurances filed with and approved by the United States Department of Health and Human Services.

Two new UGT-overexpressing cell lines were generated for the experiments outlined in this study. The UGT1A3 wild type cDNA was synthesized by standard reverse transcription using normal human liver total RNA and inserted into the pcDNA3.1/V5-His-TOPO plasmid. The sense and antisense primers used for PCR amplification of UGT1A3 were UGT1A3S (sense, 5'-AAAGCAAATGTAGCAGGCAC-3'), and UGT1A3AS (antisense, 5'-GGAAATGACTAGGGAATGGTTC-3'), corresponding to nucleotides -61 to -42 and +1635 to +1656, respectively, relative to the UGT1A3 translation start site. A UGT1A8-overexpressing cell line was previously received from Dr. Thomas Tephly (University of Iowa, Iowa City, IA; Cheng et al., 1998). While this cell line was used in previous studies of substrate glucuronidation experiments (REFS), it was recently discovered that two polymorphic variants within the UGT1A8 sequence were identified in this cell line; a T>C change at nucleotide +362, and a C>G change at nucleotide +518 (GenBank accession number NM_019076), both resulting in missense amino acid changes. A wild-type UGT1A8-over-expressing cell line was generated by reverse transcription of total RNA from the previously received cell line and subsequent PCR amplification from the cDNA using the sense and antisense primers 1A8S (sense, 5'-TTCTCTCATGGCTCGCACAGGG-3'), and 1A8AS (antisense, 5'-CTCAATGGGTCTTGGATTTGTGGGC-3'), corresponding to nucleotides -7 to +15 and +1570 to +1594, respectively, relative to the translation start site. PCR amplification for

DMD17145

both UGTs 1A3 and 1A8 was performed in a GeneAmp 9700 thermocycler (Applied Biosystems, Foster City, CA) as follows: 1 cycle of 94°C for 2 min, 35 cycles of 94°C for 30 sec, 55°C for 30 sec, and 68°C for 4 min, followed by a final cycle of 7 min at 68°C.

Site-directed mutagenesis (SDM) using the Stratagene QuikChange[®] SDM kit (La Jolla, CA) was performed for UGT1A8 to change the variant base at nucleotide +362 from the polymorphic C to the wild-type T using the primer set 1A8WTS and 1A8WTAS (sense, 5'-TTTAACTTATTTTTTTCGCATTGCAGGAG-3', and antisense, 5'-CTCCTGCAATGCGAAAAAAATAAGTTAAA-3', respectively; corresponding to nucleotides +349 to +377 relative to the translation start site – the underlined bases indicate the base-pair change). Primer set 1A8P173S and 1A8P173AS (sense, 5'-CCAGGGGAATAGCTTGCCACTATCTTG-3', and antisense, 5'-CAAGATAGTGGCAAGCTATTCCCCTGG-3', respectively, corresponding to nucleotides +506 to +532 relative to the UGT1A8 translation start site) were then used to change nucleotide +518 from G to C. SDM PCR amplification was performed as follows: and 1 cycle of 95°C for 4 min, 25 cycles of 95°C for 30 sec, 55°C for 1 min, and 68°C for 16 min, and a final cycle of 68°C for 7 min. Due to the high homology between UGT1A3 and UGT1A4, the PCR product of UGT1A3 amplification was digested with the restriction enzyme XbaI prior to gel extraction to remove co-amplified UGT1A4 PCR product. The specific PCR products of UGT1A3 (1662 bp) and UGT1A8 (1601 bp) were purified using the QIAEX[®] II gel extraction kit following electrophoresis in 1.5% agarose and subsequently sub-cloned into the pcDNA3.1/V5-His-TOPO mammalian expression vector using standard methodologies. Conformation of insert orientation was performed by restriction enzyme digestion, and UGT1A3 and UGT1A8 wild-type sequences were

DMD17145

confirmed by dideoxy sequencing of the entire PCR-amplified UGT1A3 or UGT1A8 cDNA product using two vector primers (T7 and BGH; IDT, Coralville, IA), a UGT1A3 internal anti-sense primer (UGT1A3intAS; 5'-TTCGCAAGATTCGATG-3', corresponding to nucleotides +1028 to +1046 relative to the UGT1A3 translation start site) and a UGT1A8 internal antisense primer (1A8intAS; 5'-GATAAGTTTCTCCACCACCGAC-3', corresponding to nucleotides +125 to +147 relative to the UGT1A8 translation start site). The cloned UGT1A3 and 1A8 inserts were compared to sequences described in GenBank and were confirmed to be 100% homologous to the wild-type UGT1A3 and UGT1A8 sequences.

UGT1A3 and UGT1A8-overexpressing HEK293 (human embryonic kidney fibroblast) cell lines were generated by standard electroporation techniques in the Bio-Rad GenePulser Xcell (Hercules, CA) using 10 µg of pcDNA3.1/V5-His-TOPO/UGT plasmid DNA with 5×10^6 HEK293 cells (in 0.5 mL) in serum-free DMEM media, with electroporation at 250 V and 1000 µF. Following transfection, HEK293 cells were grown in 5% CO₂ to 80% confluence in DMEM supplemented with 4.5 mM glucose, 10 mM HEPES, 10% fetal bovine serum, 100 U/mL penicillin, 100 µg/mL streptomycin and geneticin (700 µg/mL medium) for the selection of geneticin-resistant cells, with selection medium changed every 3 to 4 days. Individual UGT 1A3- and 1A8-over-expressing cell colonies were selected and monitored for UGT expression via Western blotting analysis (described below). Additional cell lines over-expressing the UGT1A and UGT2B isoforms analyzed in this study have been described previously (Ren et al., 2000; Dellinger et al., 2006; Chen et al., Submitted, 2007). All UGT overexpressing cell lines were grown in DMEM as described above. Cells were grown to 80% confluence

DMD17145

prior to the preparation of cell homogenates by re-suspending pelleted cells in Tris-buffered saline (25 mM Tris base, 138 mM NaCl, 2.7 mM KCl; pH 7.4), subjecting them to 3 rounds of freeze-thaw prior to gentle homogenization, and storage at -80°C in 100 μ L aliquots. Total homogenate protein concentrations were measured using the BCA protein assay.

Western blot analysis. Levels of UGT1A protein were determined as previously described (Dellinger et al., 2007) by our lab. UGT2B expression in UGT-over-expressing cell lines was measured by Western blot analysis using a newly-synthesized affinity-purified chicken anti-UGT2B antibody generated against the peptide CKWDQFYSEVLGRPTTL, which is common to all human UGT2B family members (Pocono Rabbit Farm, Canadensis, PA). Antibodies were used in a 1:5000 dilution. UGTs 2B7, 2B15 and 2B17 were quantified against 200 – 250 ng of human UGT2B7 protein (supplied in the Western blotting kit provided by Gentest) by densitometric analysis of X-ray film exposures (1 sec – 2 min) of Western blots using a GS-800 densitometer with Quantity One software (Bio-Rad, Hercules, CA). All cell homogenate protein levels were normalized to the levels of β -actin observed in each lane (quantified by densitometric analysis of Western blots as described above). Determinations of aglycone-Gluc formation in UGT2B7-, UGT2B15-, and UGT2B17-overexpressing cell lines were calculated relative to the levels of UGT expression in the respective cell lines. X-ray film bands were always below densitometer saturation levels as indicated by the densitometer software. Densitometric results were always consistent irrespective of the exposure time. Western blot and subsequent densitometric analysis was performed in triplicate on three separate occasions, using the same UGT-containing cell

DMD17145

homogenates used for activity assays, with relative UGT protein levels expressed as the mean of these experiments.

Synthesis of endoxifen. Using 4-OH-TAM (70:30 mixture; Sigma) as substrate, two steps were required for its conversion to endoxifen. The first step resulted in the formation of the intermediate *cis/trans*-4-OH-*N*-ethoxycarbonyl-*N*-methylTAM, with this intermediate being converted to *cis/trans*-endoxifen in the second step.

I. Synthesis of *cis/trans*-4-OH-*N*-ethoxycarbonyl-*N*-methylTAM.

Ethylchloroformate (0.05 mL) was added to a solution of 4-OH-TAM (0.10 g, 0.26 mmol) in toluene (5.0 mL) and the mixture was refluxed for 3 h. The solvent was removed under reduced pressure and the resulting crude mixture of *cis/trans* isomers was purified by silica gel column chromatography (eluant, ethyl acetate:hexanes [1:4]). The resulting *cis/trans*-4-OH-*N*-ethoxycarbonyl-*N*-methylTAM (86 mg, 74%) was confirmed by a Varian Mercury 300 MHz NMR spectrometer in CDCl₃ with tetramethylsilane as internal standard. NMR spectra were recorded using chemical shifts in ppm downfield from the internal standard. The coupling constants (*J*) are given in hertz (Hz).

¹H NMR (CDCl₃, 300 MHz) δ 0.92 (t, *J* = 7.5 Hz, 3H), 1.21-1.28 (m, 3H), 2.46 (dq, *J* = 7.5 and 2.1 Hz, 2H), 2.97 (s, 1.5H), 3.05 (s, 1.5H), 3.52-3.56 (m, 1H), 3.62-3.66 (m, 1H), 3.92-3.97 (m, 1H), 4.06-4.15 (m, 3H), 6.47 (d, *J* = 8.7 Hz, 1H), 6.51 (d, *J* = 8.4 Hz, 1H), 6.70-6.88 (m, 4H), 7.07-7.22 (m, 7H).

II. Synthesis of *cis/trans*-4-OH-*N*-desmethylTAM (*cis/trans*-endoxifen). To 4-OH-*N*-ethoxycarbonyl-*N*-methylTAM (67 mg, 0.15 mmol), ethyleneglycol (2.5 mL), hydrazine hydrate (0.25 mL), and potassium hydroxide (400 mg) were added and the resulting mixture was stirred at 140°C for 4 h. The reaction mixture was poured into ice-

DMD17145

cold water and extracted with diethyl ether. The organic layer was washed with brine, dried over anhydrous MgSO_4 and the solvent was removed under reduced pressure to yield endoxifen as a white solid (46 mg, 82%). Proton NMR of the crude mixture revealed it to be a mix of *cis* and *trans* (40:60) regio isomers. The product was further identified by LC-MS [Applied Biosystems API 150EX], with the MS spectrum resulting in a clear peak at m/z 374 $[\text{M} + \text{H}]^+$ (spectrum not shown). The *cis* and *trans* isomers of endoxifen were separated by HPLC and collected as described below. The purified *trans*- and *cis*-endoxifen was then characterized and confirmed by Bruker Avance 500 MHz NMR spectrometer: ^1H NMR ($\text{DMSO}-d_6$, 500 MHz, *trans* isomer) δ 0.85 (t, $J = 7.5$ Hz, 3H), 2.35 (s, 3H), 2.41 (q, $J = 7.5$ Hz, 2H), 2.85 (t, $J = 5.5$ Hz, 2H), 3.87 (t, $J = 5.5$ Hz, 2H), 6.58 (d, $J = 8.5$ Hz, 2H), 6.71 (d, $J = 9.0$ Hz, 2H), 6.75 (d, $J = 8.5$ Hz, 2H), 6.98 (d, $J = 8.5$ Hz, 2H), 7.08-7.12 (m, 3H), 7.16-7.20 (m, 2H), 9.41 (s, 1H, NH). ^1H NMR ($\text{DMSO}-d_6$, 500 MHz, *cis* isomer) δ 0.85 (t, $J = 7.5$ Hz, 3H), 2.40 (q, $J = 7.5$ Hz, 2H), 2.43 (s, 3H), 2.97 (t, $J = 5.5$ Hz, 2H), 4.08 (t, $J = 5.5$ Hz, 2H), 6.40 (d, $J = 8.5$ Hz, 2H), 6.60 (d, $J = 8.5$ Hz, 2H), 6.95 (d, $J = 8.5$ Hz, 2H), 7.09-7.12 (m, 5H), 7.17-7.20 (m, 2H), 9.17 (s, 1H, NH).

Separation and collection of 4-OH-TAM and endoxifen isomers. *trans*- and *cis*-4-OH-TAM, and *trans*- and *cis*-endoxifen, were separated from *trans*-/*cis*-4-OH-TAM (70:30) and *trans*-/*cis*-endoxifen (60:40) mixtures, respectively, by HPLC using a Waters 510 system (Milford, MA) equipped with an autosampler (model 717) and a UV detector operated at 254 nm (Lambda-Max model 480), with pure *trans* and *cis* isomers of both 4-OH-TAM and endoxifen individually collected after elution. HPLC was performed using a 5 μ Luna C_{18} analytical column (4.6 mm \times 250 mm, Phenomenex, Torrance,

DMD17145

CA) in series with a 5 μ C₁₈ guard column (4.0 L mm \times 3.0 ID mm; Phenomenex). For separation of *trans*- and *cis*-4-OH-TAM, the isocratic elution conditions were 20% buffer A (0.1% triethylamine, pH 7.4) and 80% acetonitrile at a 1 mL/min flow rate at room temperature. For separation of *trans*- and *cis*-endoxifen, the following isocratic conditions were 5% buffer A (0.25% triethylamine, pH 7.4) and 95% acetonitrile at a 1 mL/min flow rate with the HPLC column kept at 4°C. The collected pure *trans*- and *cis*-isomers of 4-OH-TAM and endoxifen were dried and resuspended in 100% ethanol and stored at -20°C.

Glucuronidation Assays. Glucuronidation activities of homogenates from human UGT1A and UGT2B-overexpressing cells toward *trans*- and *cis*-4-OH-TAM and *trans*- and *cis*-endoxifen were performed after an initial incubation of homogenate protein (100 μ g – 1 mg) with alamethicin (50 μ g/mg protein) for 15 min in an ice bath. Glucuronidation reactions were then performed in a final reaction volume of 100 μ L at 37°C in 50 mM Tris-HCl (pH 7.4), 10 mM MgCl₂, 4 mM UDPGA, and 1 μ M -1.4 mM TAM metabolite as indicated in the text. The range of substrate concentrations used for kinetic analysis was dependent on the K_M's obtained for each active UGT. Reactions were terminated after 60 min by the addition of 100 μ L cold methanol on ice. Mixtures were centrifuged for 10 min at 4°C at 16,100 g and the supernatants were collected and loaded onto the HPLC column.

Samples were analyzed for glucuronidated 4-OH-TAM and endoxifen metabolites by HPLC using a Beckman Coulter System Gold 126 Solvent Module HPLC system (Fullerton, CA) equipped with an automatic injector (model 508) and a UV detector operated at 254 nm (model 168). HPLC was performed using a 3 μ Luna C₁₈(2)

DMD17145

analytical column (4.6 mm \times 150 mm, Phenomenex, Torrance, CA) in series with a 5 μ m Aquasil C₁₈ guard column (10 \times 4 mm; Thermo Hypersil-Keystone, Bellefonte, PA). The gradient elution conditions for kinetic assays with *trans*- or *cis*-4-OH-TAM was as follows: starting with 75% buffer A (100 mM ammonium acetate, pH 5.0) and 25% acetonitrile, the flow rate was maintained at 0.5 mL/min over 5 min; a subsequent linear gradient to 75% acetonitrile / 25% buffer A over 25 min was performed and then maintained at 75% acetonitrile for 10 min. *trans*-4-OH-TAM-*N*⁺-glucuronide, *trans*-4-OH-TAM-O-glucuronide, *cis*-4-OH-TAM-*N*⁺-glucuronide, and *cis*-4-OH-TAM-O-glucuronide were confirmed by 1M NaOH hydrolysis and sensitivity to β -glucuronidase as previously described (Sun et al., 2006). For characterization of endoxifen glucuronides, the gradient elution conditions were the same as the gradient programs described above except that the pH of buffer A was 7.4. *trans*-endoxifen-O-glucuronide and *cis*-endoxifen-O-glucuronides were confirmed by their stability to 1M HCl treatment and their sensitivity to β -glucuronidase treatment. For kinetic assays of *trans*- or *cis*-endoxifen-O-glucuronide formation, the pH of buffer A was kept at 5.0 for better resolution, and all of the analytical conditions were the same as those for 4-OH-TAM as described above.

As controls, glucuronidation assays were regularly performed using human HLMs (as a positive control for glucuronidation activity) and untransfected HK293 cell homogenate protein (as a negative control for glucuronidation activity) as previously described (Fang et al., 2002; Wiener et al., 2004a). Experiments were always performed in triplicate in independent assays.

DMD17145

LC-MS identification of 4-OH-TAM-O-glucuronides and endoxifen-O-glucuronides. *trans*- and *cis*-4-OH-TAM-O-glucuronides were collected after separation by HPLC using a Beckman Coulter Gold 126 Solvent Module system and subsequently identified using a Shimadzu LC-MS 2010 EV system. *trans*- and *cis*-4-OH-TAM-O-glucuronides were loaded onto a Shimadzu reverse phase column (Shimadzu C18, 4.6 mm × 50 mm, Shimadzu, Tokyo, Japan) and analyzed at a flow rate of 0.2 mL/min by applying a linear mobile phase gradient from 10% to 80% (v/v) methanol/H₂O over 30 min. By using a positive mode, the electrospray voltage of 1.5 kilovolt was applied.

trans- and *cis*-endoxifen-O-glucuronides were identified using an Applied Biosystems LC/MS/MS system. *trans*- and *cis*-endoxifen-O-glucuronides were loaded onto a C18 column (Aquasil C18, 2.1 mm × 150 mm, 3 μ, Thermo, PA, USA) and subsequently analyzed at a flow rate of 0.2 mL/min by applying a mobile phase gradient from 5% to 100% (v/v) methanol/acetic acid. By using a positive mode, the electrospray voltage of 2.5 kilovolt was applied.

Statistical Analysis. The Student's t-test (2-sided) was used for comparing rates and kinetic values of glucuronide formation for individual UGT1A and UGT2B enzymes against the different substrates examined in this study. Kinetic constants were determined using Graphpad Prism4 software.

DMD17145

Results

Synthesis of endoxifen. Previous reports examining endoxifen metabolism and activity involved multi-step synthesis (Burke and Koch, 2004). In the present study, a two-step synthesis of endoxifen by the demethylation of 4-OH-TAM has been developed as outlined in Figure 1. Treatment of 4-OH-TAM (**1**) with ethylchloroformate in refluxing toluene gave the intermediate (**2**) as an isomeric mixture of *cis/trans* isomers. The treatment of the mixture (**2**) with hydrazine hydrate in the presence of ethylene glycol and potassium hydroxide led to a mixture (60:40) of geometrical *cis/trans* isomers of endoxifen (**3**).

The regio-isomeric mixture (**3**) was characterized on the basis of ^1H NMR and mass spectra. The MS spectrum of the *trans/cis* mixture (**3**) showed a clear $[\text{M}+\text{H}]^+$ peak at m/z 374 (the molecular weight of endoxifen is 373). The ratio of the mixture was assigned on the basis of the integration of the $-\text{NCH}_3$ protons by NMR (δ 2.35, *trans* isomer and 2.40, *cis* isomer) and HPLC of the crude mixture. The *trans* and *cis* configuration was assigned to the separated isomers of endoxifen on the basis of their ^1H NMR chemical shift profile in accordance with the literature reports (Shani et al., 1985; Ogawa et al., 1991). The chemical shift of triplets for $-\text{OCH}_2$ proton in ^1H NMR spectra appeared at δ 3.87 and 4.08 ppm, respectively. Based on previous studies (Shani et al., 1985; Ogawa et al., 1991), the chemical shifts of the *cis* isomer, where the $-\text{OCH}_2$ substituent is situated *trans* to the aryl ring, are shifted to the lower field than those in the *trans*-form. Based on this information, the isomer having the triplet at δ 4.08

DMD17145

was assigned as the *cis*-isomer (40%) and the one with δ 3.87 was identified as the *trans*-isomer (60%).

Separation and collection of 4-OH-TAM and endoxifen isomers. As described in the Materials and methods, isocratic HPLC elution programs were developed to efficiently separate 4-OH-TAM and endoxifen isomers. Due to relatively high level of intra-conversion between *trans*- and *cis*-4-OH-TAM as well as *trans*- and *cis*-endoxifen under acidic condition, the separation buffer was maintained at pH7.4 using triethylamine. As shown in Figure 2, the *trans* (peak 1) and *cis* isomers (peak 2) of 4-OH-TAM eluted in HPLC of a 70%:30% mix of *trans*:-*cis*-4-OH-TAM (panel A), 98% pure *trans*-4-OH-TAM purchased from Sigma Co. (panel B), and collected pure *cis*-4-OH-TAM (panel C), at retention times of 16.6 and 19.9 min, respectively. Two peaks were also observed for the newly-synthesized, NMR-confirmed endoxifen mixture, eluting at 8.5 min (peak 3) and 10.5 min (peak 4) with a peak 3:peak4 area ratio of 60:40 (panel D). Collected peaks 3 (panel E) and 4 (panel F) were characterized and confirmed by proton NMR data which indicated that peaks 3 and 4 were *trans*- and *cis*-endoxifen, respectively. Therefore, the pattern of shorter retention time for the *trans*- versus *cis*-isomers was consistent for both TAM metabolites by HPLC. The purified, collected *trans*- and *cis*-4-OH-TAM and *trans*- and *cis*-endoxifen were stable in ethanol and used for glucuronidation assays described below.

Characterization of 4-OH-TAM-O-glucuronides. Previous studies have demonstrated that HLMS catalyze the glucuronidation of 4-OH-TAM to both the O-glucuronide and *N*⁺-glucuronide forms for both its *trans*- and *cis*-isomers, and that UGT1A4 is the major enzyme responsible for forming 4-OH-TAM-*N*⁺-glucuronide (Sun

DMD17145

et al., 2006). To identify the UGTs responsible for O-glucuronidation of 4-OH-TAM isomers, cell lines overexpressing UGTs 1A1, 1A3, 1A4, 1A6, 1A7, 1A8, 1A9, 1A10, 2B4, 2B7, 2B10, 2B11, 2B15 and 2B17 were examined. Similar to that observed in previous study (Sun et al., 2006), the O- and *N*⁺-glucuronides of *trans*-4-OH-TAM formed in assays with HLMs eluted with elution times of 18.2 min (peak 1) and 23 min (peak 2), respectively (Figure 3, panel A); a similar pattern was observed for *cis*-4-OH-TAM, with retention times of 18.6 min (peak 4) and 22.5 min (peak 5) for the respective O- and *N*⁺-glucuronides (panel B). In assays with UGT-overexpressing cell homogenates, single glucuronide peaks corresponding to the retention times of peak 1 and peak 4 were observed in assays with *trans*- and *cis*-4-OH-TAM, respectively, for several UGTs including UGT2B7 (panel C and D). Similar to that observed previously (Sun et al., 2006), peaks 1 and 4 were not alkali-sensitive but were sensitive to treatment with β -glucuronidase (results not shown), suggesting that these glucuronides were the O-glucuronides of 4-OH-TAM isomers. The products corresponding to the predicted *trans*- and *cis*-4-OH-TAM-O-glucuronides were collected and analyzed using LC with electrospray MS detection. The mass spectrum for the *trans*-4-OH-TAM-O-glucuronide (with a calculated molecular weight of 563.29) showed a clear [M⁺] ion at *m/z* 563.75 (Figure 3, panel E). A virtually identical pattern was observed for *cis*-4-OH-TAM-O-glucuronide with a clear [M⁺] ion at *m/z* 563.80 (data not shown). These data suggest that the glucuronides derived from both isomers were in fact monoglucuronides.

UGT1A3 was the only UGT tested in this analysis to form two glucuronide peaks (peak 1 and 2) against 4-OH-TAM, and this was specific for the *trans*-isomer (results not

DMD17145

shown). Like the peak 2 formed by HLMs (Figure 3, panel A), UGT1A3-catalyzed peak 2 was sensitive to both 1M NaOH and β -glucuronidase treatment (results not shown). Similar to that reported previously (Sun et al., 2006), UGT1A4 only formed *N*⁺-glucuronides against both the *trans* and *cis* isomers of 4-OH-TAM; no O-glucuronides were observed against 4-OH-TAM isomers. Of the UGTs tested, only 1A6, 2B4, 2B10 and 2B11 did not exhibit detectable glucuronidation activity against both isomers of 4-OH-TAM.

Characterization of endoxifen glucuronides. Single putative glucuronide peaks with retention times of 17.9 min (peak 1) and 18.4 min (peak 3) were observed in assays of HLMs (Figure 4, panels A and B) or UGT-overexpressing cell homogenates including UGT1A10 (panels C and D) with either *trans*-endoxifen or *cis*-endoxifen, respectively. Both peaks were stable after incubations with 1M HCl overnight but were sensitive to treatment with β -glucuronidase (results not shown), suggesting that both glucuronide peaks were the O-glucuronide conjugates of *trans*- and *cis*-endoxifen, respectively. The products corresponding to the predicted *trans*- and *cis*-endoxifen-O-glucuronides were collected and analyzed by LC/MS/MS detection (Figure 4, panel E). The mass spectrum for the *trans*-endoxifen-O-glucuronide (with a calculated molecular weight of 549.2) showed a clear [M⁺] ion at *m/z* 550.2 and a fragment ion at *m/z* 374.2, the latter corresponding to the parent drug endoxifen +H with the loss of the glucuronide acid moiety (molecular weight = 176 g/mol; Figure 4, panel E). A virtually identical pattern was observed for *cis*-endoxifen-O-glucuronide with a clear [M⁺] ion at *m/z* 550.7 (data not shown). These data suggest that the glucuronides derived from both isomers were in fact monoglucuronides.

DMD17145

Since endoxifen is a secondary amine, potential endoxifen-*N*-glucuronides may be sensitive to acid treatment. For optimal resolution of 4-OH-TAM and endoxifen isomers, the HPLC gradient used in the present kinetic study was pH 5.0. It is possible that endoxifen-*N*-glucuronides were de-conjugated during the HPLC elution process at this pH since *N*-glucuronides of secondary amines are susceptible to cleavage under mildly acidic conditions (Babu et al., 1992). When assays were run on a HPLC gradient at pH 7.4, only single glucuronide peaks corresponding to peaks 1 and 3 (for *trans*- and *cis*-endoxifen, respectively) were observed for both HLMs and UGT-overexpressing cell, and these glucuronide peaks were stable in 1M HCl but sensitive to β -glucuronidase treatment (data not shown). These data indicated that these single peaks were in fact endoxifen-*O*-glucuronides and that no endoxifen-*N*-glucuronides formation was observed in assays with endoxifen.

Kinetic analysis of 4-OH-TAM and endoxifen glucuronidation by human

UGTs. In addition to the newly-made UGT1A3 and UGT1A8 cell lines described in this report, cell lines overexpressing UGTs 1A1, 1A4, 1A6, 1A7, 1A9, 1A10, 2B4, 2B7, 2B10, 2B11, 2B15 and 2B17 were used for this analysis as previously described (Babu et al., 1992; Chen et al., Submitted, 2007). Of the UGTs tested in this study, UGTs 1A1, 1A3, 1A7, 1A8, 1A9, 1A10, 2B7, 2B15 and 2B17 exhibited detectable levels of *O*-glucuronidating activity against *trans*- and *cis*-4-OH-TAM. UGT1A4 selectively exhibited *N*⁺-glucuronidating activity against both 4-OH-TAM isomers in this as well as in previous studies (Sun et al., 2006). UGTs 1A6, 2B4, 2B10 and 2B11 did not exhibit detectable glucuronidating activity against either 4-OH-TAM isomer. After normalizing for UGT1A protein expression as determined by Western blot analysis (Dellinger et al., Submitted),

DMD17145

the order of O-glucuronidation activity of the *trans*-4-OH-TAM isomer based upon V_{\max}/K_M was $1A8 > 1A10 > 1A1 > 1A3 > 1A9 \geq 1A7$. A newly-designed anti-UGT2B antibody (described in the Materials and methods) was reactive against UGTs 2B7, 2B15 and 2B17 (Figure 5). After normalizing for UGT2B protein expression, the order of O-glucuronidation activity of the *trans*-4-OH-TAM isomer based upon V_{\max}/K_M was $2B7 \gg 2B17$. For the *cis* isomer of 4-OH-TAM, the order of O-glucuronidation activity based upon V_{\max}/K_M was $1A10 > 1A1 > 1A8 > 1A9 > 1A3 \geq 1A7$ for the UGT1A family and $2B7 > 2B15 > 2B17$ for the UGT2B family. Overall, the UGT2B family members exhibited the lowest K_M 's against 4-OH-TAM, with UGTs 2B7 (3.7 and 14.8 μM) and 2B17 (40.6 and 18 μM) exhibiting high affinity for the *trans* and *cis* isomers, respectively. Of the family 1A UGTs, 1A8 exhibited the lowest K_M (22.7 μM) against *trans*-4-OH-TAM and 1A7 exhibited the lowest (7.4 μM) against *cis*-4-OH-TAM.

Of the UGTs tested in this study, UGT1A3 was the only enzyme exhibiting both O- and *N*⁺-glucuronidation activity against 4-OH-TAM. The K_M and V_{\max}/K_M of UGT1A3 for *trans*-4-OH-TAM-*N*⁺-glucuronide formation were 193 μM and 0.005 $\mu l \cdot min^{-1} \cdot \mu g^{-1}$; no detectable *N*⁺-glucuronidation activity was observed by UGT1A3 against *cis*-4-OH-TAM.

Of the UGT-overexpressing cell lines tested, the highest overall O-glucuronidating activities against *trans*-endoxifen by UGT family 1A enzymes as determined by kinetic analysis (V_{\max}/K_M) were $1A10 > 1A8 > 1A3 > 1A1 > 1A7 \approx 1A9$ for *trans*-endoxifen, and $1A10 > 1A9 > 1A3 > 1A8 > 1A7 > 1A1$ for *cis*-endoxifen. Unlike the N-glucuronide formation observed for isomers of 4-OH-TAM, no glucuronides were formed by homogenates of UGT1A4-overexpressing cells against both isomers of endoxifen. The only UGT2B enzyme that exhibited O-glucuronidation activity against

DMD17145

trans-endoxifen was 2B7. The order of O-glucuronidation activity against *cis*-endoxifen for the UGT2B enzymes was 2B15 > 2B7 > 2B17. Overall, UGT1A10 exhibited the lowest K_M against both *trans*- (39.9 μ M) and *cis*-endoxifen (11.2 μ M). No endoxifen-*N*-glucuronide formation was observed by any UGT screened in this study including UGT1A4. As exhibited for 4-OH-TAM isomers, UGTs 1A6, 2B4, 2B10 and 2B11 exhibited no detectable glucuronidation activity against either endoxifen isomer.

DMD17145

Discussion

Limited studies had previously been reported identifying the UGT enzymes involved in TAM metabolism. UGT1A4 was shown to be the major enzyme involved in *N*⁺-glucuronidation of TAM and both isomers of 4-OH-TAM (Sun et al., 2006). The *N*⁺-glucuronidation activity exhibited by UGT1A4 to form a quarternary ammonium-linked glucuronide with TAM's *N,N*-dimethylaminoalkyl side chain is consistent with UGT1A4's activity spectrum to produce *N*⁺-glucuronidated metabolites with other compounds (Green and Tephly, 1998; Ren et al., 1999; Wiener et al., 2004a). In the present study, UGT1A3 also exhibited *N*⁺-glucuronidation activity, but only for the *trans* isomer of 4-OH-TAM and at relatively low levels. This is consistent with the dual activities observed for UGT1A3 against other substrates (Green and Tephly, 1998).

While UGT2B15 was shown in previous studies to be active against *cis*-4-OH-TAM (Ogura et al., 2006), the present study is the first to perform a comprehensive analysis of *O*-glucuronidation of 4-OH-TAM and is the first to examine endoxifen glucuronidation. In addition, this is the first report to examine the pure *trans* and *cis*-endoxifen isomers independently. Using an optimized synthesis strategy based on the methodology described by Kitagawa *et al.* (Kitagawa et al., 2000), large amounts of endoxifen were synthesized for these studies, with the *trans* and *cis* isomers separated and purified for kinetic analysis. Both isomers of endoxifen are *O*-glucuronidated, however, unlike 4-OH-TAM, no *N*-glucuronidation of endoxifen isomers was detected in our assays for either liver microsomes or individually-overexpressed UGTs including

DMD17145

UGT1A4, suggesting that the demethylation of the electrophilic amine on the 4-OH-TAM side chain results in a lack of *N*-glucuronidation by UGTs.

Kinetic analysis suggests that UGT2B7 is the major hepatic enzyme responsible for the *O*-glucuronidation of the *trans* isomer of both 4-OH-TAM and endoxifen. This was reflected by a relatively high V_{\max}/K_M and low apparent K_M as compared to other hepatic UGTs against the two TAM metabolites. Of the extra-hepatic UGTs, both 1A8 and 1A10 exhibited significant *O*-glucuronidation activity against the *trans* isomer of 4-OH-TAM and endoxifen, with UGT1A10 exhibiting the lowest K_M of any UGT against *trans*-endoxifen.

Like that observed for the *trans* isomers, UGT1A10 also exhibited significant levels of *O*-glucuronidation activity against *cis*-4-OH-TAM and *cis*-endoxifen, exhibiting 10-24-fold higher levels of activity as determined by V_{\max}/K_M than any other UGT examined. However, some regio-isomeric specificity was apparent in terms of UGT activity relationships against the different isomers of the two TAM metabolites. UGT1A9, which exhibited only low levels of activity against their respective *trans* isomers, exhibited *O*-glucuronidation activity that was similar to or greater than that observed for UGT1A8 against the *cis* isomers of both 4-OH-TAM or endoxifen. Similarly, UGTs 2B15 and 2B17, which exhibited low or undetectable levels of activity against both *trans*-4-OH-TAM and *trans*-endoxifen, exhibited similar or greater *O*-glucuronidation activity against the *cis* isomers of both TAM metabolites to that exhibited by UGT2B7, activities that were similar to the levels observed for UGT1A8 against the *cis* TAM metabolites. The K_M 's of UGTs 2B15 and 2B17 were amongst the lowest observed for any UGT against *cis*-4-OH-TAM. In addition, while exhibiting low *O*-glucuronidation activity

DMD17145

against the *trans* isomers and *cis*-endoxifen, UGT1A1 exhibited a level of activity that was amongst the highest of all hepatic UGTs as determined by V_{\max}/K_M against *cis*-4-OH-TAM. Therefore, while it is likely that UGTs 1A10 and 2B7 play an important overall role in hepatic and potentially extra-hepatic elimination of 4-OH-TAM and endoxifen, there is significant cross-reactivity with other UGTs for the different isomeric forms of the two TAM metabolites.

While several of the UGTs highly active against 4-OH-TAM and endoxifen isomers are hepatic including UGT2B7, several are also expressed in target tissues for TAM response including breast [(Lepine et al., 2004); our unpublished results], including UGT2B7 and the extra-hepatic UGTs 1A8 and 1A10. The presence of all three in breast could be important in the local elimination of TAM metabolites in this target tissue.

In summary, results from this study indicate that UGTs 2B7, 1A8 and 1A10 were highly active against *trans*-4-OH-TAM and *trans*-endoxifen. UGTs 1A10, 1A8, 2B7 and 2B15 were highly active against *cis*-4-OH-TAM, while UGT1A10 exhibited the highest O-glucuronidating activity against *cis*-endoxifen. These UGTs are expressed in human liver and/or breast, and alterations in their expression or activity including genetic variation could therefore potentially impact TAM related treatment efficacy. Studies are currently underway examining functional polymorphisms in these active enzymes and their potential role in overall response to TAM.

DMD17145

References

- (1998) Tamoxifen for early breast cancer: an overview of the randomised trials. Early Breast Cancer Trialists' Collaborative Group. *Lancet* **351**:1451-1467.
- Babu SR, Lakshmi VM, Hsu FF, Zenser TV and Davis BB (1992) Role of N-glucuronidation in benzydine-induced bladder cancer in dog. *Carcinogenesis* **13**:1235-1240.
- Bergman L, Beelen ML, Gallee MP, Hollema H, Benraadt J and van Leeuwen FE (2000) Risk and prognosis of endometrial cancer after tamoxifen for breast cancer. Comprehensive Cancer Centres' ALERT Group. Assessment of Liver and Endometrial cancer Risk following Tamoxifen. *Lancet* **356**:881-887.
- Burke PJ and Koch TH (2004) Design, synthesis, and biological evaluation of doxorubicin-formaldehyde conjugates targeted to breast cancer cells. *J Med Chem* **47**:1193-1206.
- Chowdhury S and Ellis P (2005) Extended adjuvant endocrine therapy of early breast cancer. *Curr Med Res Opin* **21**:1985-1995.
- Coughtrie MW, Burchell B and Bend JR (1986) A general assay for UDPglucuronosyltransferase activity using polar amino-cyano stationary phase HPLC and UDP[U-14C]glucuronic acid. *Anal Biochem* **159**:198-205.
- Cuzick J, Powles T, Veronesi U, Forbes J, Edwards R, Ashley S and Boyle P (2003) Overview of the main outcomes in breast-cancer prevention trials. *Lancet* **361**:296-300.
- Dellinger RW, Chen G, Blevins-Primeau AS, Krzeminski J, Amin S and Lazarus P Glucuronidation of PhIP and N-OH-PhIP by UDP-glucuronosyltransferase 1A10.

DMD17145

Carcinogenesis (In Press).

Dellinger RW, Fang JL, Chen G, Weinberg R and Lazarus P (2006) Importance of UDP-glucuronosyltransferase 1A10 (UGT1A10) in the detoxification of polycyclic aromatic hydrocarbons: decreased glucuronidative activity of the UGT1A10^{139lys} isoform. *Drug Metab Dispos* **34**:943-949.

Fang JL, Beland FA, Doerge DR, Wiener D, Guillemette C, Marques MM and Lazarus P (2002) Characterization of benzo(a)pyrene-trans-7,8-dihydrodiol glucuronidation by human tissue microsomes and overexpressed UDP-glucuronosyltransferase enzymes. *Cancer Res* **62**:1978-1986.

Fisher B, Costantino JP, Redmond CK, Fisher ER, Wickerham DL and Cronin WM (1994) Endometrial cancer in tamoxifen-treated breast cancer patients: findings from the National Surgical Adjuvant Breast and Bowel Project (NSABP) B-14. *J Natl Cancer Inst* **86**:527-537.

Fisher B, Costantino JP, Wickerham DL, Redmond CK, Kavanah M, Cronin WM, Vogel V, Robidoux A, Dimitrov N, Atkins J, Daly M, Wieand S, Tan-Chiu E, Ford L and Wolmark N (1998) Tamoxifen for prevention of breast cancer: report of the National Surgical Adjuvant Breast and Bowel Project P-1 Study. *J Natl Cancer Inst* **90**:1371-1388.

Green MD and Tephly TR (1998) Glucuronidation of amine substrates by purified and expressed UDP-glucuronosyltransferase proteins. *Drug Metab Dispos* **26**:860-867.

Howell A, Howell SJ and Evans DG (2003) New approaches to the endocrine prevention and treatment of breast cancer. *Cancer Chemother Pharmacol* **52**

DMD17145

Suppl 1:S39-44.

- Jordan VC, Collins MM, Rowsby L and Prestwich G (1977) A monohydroxylated metabolite of tamoxifen with potent antioestrogenic activity. *J Endocrinol* **75**:305-316.
- Kaku T, Ogura K, Nishiyama T, Ohnuma T, Muro K and Hiratsuka A (2004) Quaternary ammonium-linked glucuronidation of tamoxifen by human liver microsomes and UDP-glucuronosyltransferase 1A4. *Biochem Pharmacol* **67**:2093-2102.
- Kitagawa M, Ravindernath A, Suzuki N, Rieger R, Terashima I, Umemoto A and Shibutani S (2000) Identification of tamoxifen-DNA adducts induced by alpha-acetoxy-N-desmethyltamoxifen. *Chem Res Toxicol* **13**:761-769.
- Lepine J, Bernard O, Plante M, Tetu B, Pelletier G, Labrie F, Belanger A and Guillemette C (2004) Specificity and regioselectivity of the conjugation of estradiol, estrone, and their catecholestrogen and methoxyestrogen metabolites by human uridine diphospho-glucuronosyltransferases expressed in endometrium. *J Clin Endocrinol Metab* **89**:5222-5232.
- Lien EA, Solheim E, Lea OA, Lundgren S, Kvinnsland S and Ueland PM (1989) Distribution of 4-hydroxy-N-desmethyltamoxifen and other tamoxifen metabolites in human biological fluids during tamoxifen treatment. *Cancer Res* **49**:2175-2183.
- Lim YC, Desta Z, Flockhart DA and Skaar TC (2005) Endoxifen (4-hydroxy-N-desmethyl-tamoxifen) has anti-estrogenic effects in breast cancer cells with potency similar to 4-hydroxy-tamoxifen. *Cancer Chemother Pharmacol* **55**:471-478.
- McDonald CC and Stewart HJ (1991) Fatal myocardial infarction in the Scottish

DMD17145

- adjuvant tamoxifen trial. The Scottish Breast Cancer Committee. *Bmj* **303**:435-437.
- Meier CR and Jick H (1998) Tamoxifen and risk of idiopathic venous thromboembolism. *Br J Clin Pharmacol* **45**:608-612.
- Murphy CS, Langan-Fahey SM, McCague R and Jordan VC (1990) Structure-function relationships of hydroxylated metabolites of tamoxifen that control the proliferation of estrogen-responsive T47D breast cancer cells in vitro. *Mol Pharmacol* **38**:737-743.
- Nechushtan H and Peretz T (2002) [Tamoxifen and breast cancer]. *Harefuah* **141**:718-720, 761, 760.
- Nishiyama T, Ogura K, Nakano H, Ohnuma T, Kaku T, Hiratsuka A, Muro K and Watabe T (2002) Reverse geometrical selectivity in glucuronidation and sulfation of cis- and trans-4-hydroxytamoxifens by human liver UDP-glucuronosyltransferases and sulfotransferases. *Biochem Pharmacol* **63**:1817-1830.
- Nowell SA, Ahn J, Rae JM, Scheys JO, Trovato A, Sweeney C, MacLeod SL, Kadlubar FF and Ambrosone CB (2005) Association of genetic variation in tamoxifen-metabolizing enzymes with overall survival and recurrence of disease in breast cancer patients. *Breast Cancer Res Treat* **91**:249-258.
- Ogawa K, Matsushita Y, Yamawaki I, Kaneda M, Shibata J, Toko T and Asao T (1991) Synthesis and antiestrogenic activity of the compounds related to the metabolites of (E)-4-[1-[4-[2-(dimethylamino)ethoxy]phenyl]-2-(4-isopropylphenyl)-1-butenyl]phenyl monophosphate (TAT-59) [corrected]. *Chem Pharm Bull (Tokyo)*

DMD17145

39:911-916.

Ogura K, Ishikawa Y, Kaku T, Nishiyama T, Ohnuma T, Muro K and Hiratsuka A (2006)

Quaternary ammonium-linked glucuronidation of trans-4-hydroxytamoxifen, an active metabolite of tamoxifen, by human liver microsomes and UDP-glucuronosyltransferase 1A4. *Biochem Pharmacol* **71**:1358-1369.

Osborne CK (1998) Tamoxifen in the treatment of breast cancer. *N Engl J Med*

339:1609-1618.

Poon GK, Chui YC, McCague R, Llinning PE, Feng R, Rowlands MG and Jarman M

(1993) Analysis of phase I and phase II metabolites of tamoxifen in breast cancer patients. *Drug Metab Dispos* **21**:1119-1124.

Ren Q, Murphy SE, Dannenberg AJ, Park JY, Tephly TR and Lazarus P (1999)

Glucuronidation of the lung carcinogen 4-(methylnitrosamino)-1-(3-pyridyl)-1-butanol (NNAL) by rat UDP-glucuronosyltransferase 2B1. *Drug Metab Dispos* **27**:1010-1016.

Ren Q, Murphy SE, Zheng Z and Lazarus P (2000) O-Glucuronidation of the lung

carcinogen 4-(methylnitrosamino)-1-(3-pyridyl)-1-butanol (NNAL) by human UDP-glucuronosyltransferases 2B7 and 1A9. *Drug Metab Dispos* **28**:1352-1360.

Robertson DW, Katzenellenbogen JA, Long DJ, Rorke EA and Katzenellenbogen BS

(1982) Tamoxifen antiestrogens. A comparison of the activity, pharmacokinetics, and metabolic activation of the cis and trans isomers of tamoxifen. *J Steroid Biochem* **16**:1-13.

Rutqvist LE and Mattsson A (1993) Cardiac and thromboembolic morbidity among

postmenopausal women with early-stage breast cancer in a randomized trial of

DMD17145

adjuvant tamoxifen. The Stockholm Breast Cancer Study Group. *J Natl Cancer Inst* **85**:1398-1406.

Shani J, Gazit A, Livshitz T and Biran S (1985) Synthesis and receptor-binding affinity of fluorotamoxifen, a possible estrogen-receptor imaging agent. *J Med Chem* **28**:1504-1511.

Sun D, Chen G, Dellinger RW, Duncan K, Fang JL and Lazarus P (2006) Characterization of tamoxifen and 4-hydroxytamoxifen glucuronidation by human UGT1A4 variants. *Breast Cancer Res* **8**:R50.

van Leeuwen FE, Benraadt J, Coebergh JW, Kiemeney LA, Gibrere CH, Otter R, Schouten LJ, Damhuis RA, Bontenbal M, Diepenhorst FW and et al. (1994) Risk of endometrial cancer after tamoxifen treatment of breast cancer. *Lancet* **343**:448-452.

Wiener D, Doerge DR, Fang JL, Upadhyaya P and Lazarus P (2004a) Characterization of N-glucuronidation of the lung carcinogen 4-(methylnitrosamino)-1-(3-pyridyl)-1-butanol (NNAL) in human liver: importance of UDP-glucuronosyltransferase 1A4. *Drug Metab Dispos* **32**:72-79.

Wiener D, Fang JL, Dossett N and Lazarus P (2004b) Correlation between UDP-glucuronosyltransferase genotypes and 4-(methylnitrosamino)-1-(3-pyridyl)-1-butanone glucuronidation phenotype in human liver microsomes. *Cancer Res* **64**:1190-1196.

DMD17145

Footnotes

These studies were supported by Public Health Service (PHS) P01-68384 (National Cancer Institute) from the National Institutes of Health, Department of Health and Human Services to P. Lazarus, and a formula grant under the Pennsylvania Department of Health's Health Research Formula Funding Program (State of PA, Act 2001-77 – part of the PA Tobacco Settlement Legislation) to P. Lazarus.

Philip Lazarus, Ph.D., Penn State Cancer Institute, Penn State University College of Medicine, Rm. C3739D, MC-H069, 500 University Drive, Hershey, PA 17033. Tel: (717)-531-5734; Fax: (717) 531-0480; Email: plazarus@psu.edu

DMD17145

Figure Legends

Figure 1. Schematic for endoxifen synthesis. Reagents and conditions: (i) ClCOOEt, toluene, reflux, 3 h; (ii) KOH, NH₂NH₂, HOCH₂CH₂OH, 140°C, 4h, as described in the Materials and Methods.

Figure 2. Separation and collection of 4-OH-TAM and endoxifen isomers by HPLC. Separation and collection was performed by HPLC as described in the Materials and Methods. Panel **A**, 70:30 mixture of *trans*-4-OH-TAM:*cis*-4-OH-TAM purchased from Sigma; panel **B**, 98% pure *trans*-4-OH-TAM purchased from Sigma; panel **C**, *cis*-4-OH-TAM purified from 70:30 mixture shown in panel A; panel **D**, 60:40 mixture of newly-synthesized (see Figure 1) *trans*-endoxifen:*cis*-endoxifen; panel **E**, *trans*-endoxifen purified from 60:40 mixture shown in panel D; panel **F**, *cis*-endoxifen purified from 60:40 mixture shown in panel D. Peak 1, *trans*-4-OH-TAM; peak 2, *cis*-4-OH-TAM; peak 3, *trans*-endoxifen; peak 4, *cis*-endoxifen.

Figure 3. HPLC and MS analysis of 4-OH-TAM-glucuronides. Glucuronidation assays were performed and 4-OH-TAM-glucuronides separated by HPLC as described in the Materials and Methods. HLMS (10 µg protein, panels **A** and **B**) or UGT2B7-overexpressing cell homogenates (500 µg of protein, panels **C** and **D**) were incubated at 37°C for 60 min with *trans*-4-OH-TAM (50 µM for panel **A** and 16 µM for panel **C**), or with *cis*-4-OH-TAM (50 µM for panel **B** and 25 µM for panel **D**), and 4 mM UDPGA prior to analysis by HPLC. Peak 1, *trans*-4-OH-TAM-O-glucuronide; peak 2, *trans*-4-OH-TAM-*N*⁺-glucuronide; peak 3, *trans*-4-OH-TAM; peak 4, *cis*-4-OH-TAM-O-glucuronide;

DMD17145

peak 5, *cis*-4-OH-TAM-*N*⁺-glucuronide; peak 6, *cis*-4-OH-TAM. Panel **E**, MS analysis of *trans*-4-OH-TAM-O-glucuronide formed by HLMs.

Figure 4. HPLC and MS analysis of endoxifen-glucuronides. Glucuronidation assays were performed and endoxifen-glucuronides separated by HPLC as described in the Materials and Methods. HLMs (30 µg protein, panels **A** and **B**) or UGT1A10-overexpressing cell homogenates (100 µg of protein, panels **C** and **D**) were incubated at 37°C for 60 min with 50 µM *trans*-endoxifen (panels **A** and **B**) or *cis*-endoxifen (panel **C** and **D**) and 4 mM UDPGA prior to analysis by HPLC. Peak 1, *trans*-endoxifen-O-glucuronide; peak 2, *trans*-endoxifen; peak 3, *cis*-endoxifen-O-glucuronide; peak 4, *cis*-endoxifen. Panel **E**, MS analysis of *trans*-endoxifen-O-glucuronide formed by HLMs.

Figure 5. Analysis of UGT2B expression. Representative Western blot analysis of UGT2B protein levels in homogenate lysates from the individual UGT-overexpressing cell lines used in the glucuronidation activity analysis against 4-OH-TAM and endoxifen. UGTs2B7, 2B15 and 2B17 protein levels were calculated against known amounts of UGT2B7 standard protein (from Gentest) with quantification made relative to the levels of β-actin observed in each lane. UGT2B7 Std 1, 200 ng UGT2B7 protein, UGT2B7 Std 2, 250 ng UGT2B7 protein. 20 µg of homogenate protein were loaded in each lane for UGTs 2B7-, 2B15- and 2B17-overexpressing cells. The negative control HEK293 (20 µg homogenate protein) lane shows no UGT1A expression in the parental HEK293 cells.

Table 1. Kinetic analysis of UGTs-induced O-glucuronidation of *trans*- and *cis*-4-OH-TAM^{a,b}

UGT	<i>trans</i> -4-OH-TAM			<i>cis</i> -4-OH-TAM		
	V_{\max} (pmol·min ⁻¹ ·μg ⁻¹)	K_M (μM)	V_{\max}/K_M (μl·min ⁻¹ ·μg ⁻¹)	V_{\max} (pmol·min ⁻¹ ·μg ⁻¹)	K_M (μM)	V_{\max}/K_M (μl·min ⁻¹ ·μg ⁻¹)
1A1	3.4 ± 0.2	124 ± 16	0.028 ± 0.004	24.6 ± 3.5	193 ± 26	0.13 ± 0.017
1A3	1.9 ± 0.3	93.7 ± 17.7	0.020 ± 0.001	6.0 ± 0.5	165 ± 26	0.036 ± 0.008*
1A7	1.2 ± 0.2	166 ± 27	0.0074 ± 0.0002	0.20 ± 0.03	7.4 ± 1.3	0.027 ± 0.001
1A8	3.2 ± 0.2	22.7 ± 2.4	0.14 ± 0.02	4.9 ± 0.2	56.1 ± 9.1	0.088 ± 0.011
1A9	3.0 ± 0.1	319 ± 38	0.009 ± 0.001	4.9 ± 1.1	69.9 ± 19.3	0.071 ± 0.005
1A10	4.7 ± 0.3	96.1 ± 7.7	0.049 ± 0.006	35.3 ± 0.2	30.0 ± 5.1	1.20 ± 0.20
2B7	0.55 ± 0.18	3.7 ± 0.6	0.15 ± 0.03	1.8 ± 0.6	14.8 ± 4.5	0.12 ± 0.02
2B15	not detectable			1.6 ± 0.2	19.6 ± 1.1	0.08 ± 0.01
2B17	0.017 ± 0.001	40.6 ± 6.2	0.001 ± 0.0001	0.21 ± 0.02	18.0 ± 2.1	0.012 ± 0.001

^a All data are the mean ± SD based on three independent experiments.

^b Homogenates from cells overexpressing UGTs 1A6, 2B4, 2B10 or 2B11 exhibited no detectable glucuronidating activity against 4-OH-TAM.

Table 2. Kinetic analysis of UGTs-induced O-glucuronidation of *trans*- and *cis*-endoxifen^{a,b}

UGT	<i>trans</i> -endoxifen			<i>cis</i> -endoxifen		
	V_{\max} (pmol·min ⁻¹ ·μg ⁻¹)	K_M (μM)	V_{\max}/K_M (μl·min ⁻¹ ·μg ⁻¹)	V_{\max} (pmol·min ⁻¹ ·μg ⁻¹)	K_M (μM)	V_{\max}/K_M (μl·min ⁻¹ ·μg ⁻¹)
1A1	2.3 ± 0.3	333 ± 60	0.0069 ± 0.0005	low activity ^c		
1A3	2.9 ± 0.4	158 ± 29	0.018 ± 0.001	19.0 ± 4.0	251 ± 97	0.08 ± 0.01
1A7	low activity			1.8 ± 0.1	68.9 ± 3.8	0.026 ± 0.001
1A8	11.6 ± 1.4	101 ± 13	0.12 ± 0.01	7.1 ± 1.0	201 ± 53	0.036 ± 0.005
1A9	low activity			7.2 ± 0.3	56.0 ± 3.3	0.13 ± 0.01
1A10	5.7 ± 0.7	39.9 ± 3.4	0.14 ± 0.005	34.2 ± 3.3	11.2 ± 0.9	3.1 ± 0.2
2B7	3.0 ± 0.4	101 ± 17	0.030 ± 0.004	2.1 ± 0.3	120 ± 22	0.018 ± 0.001
2B15	not detectable			1.4 ± 0.1	32.7 ± 6.4	0.044 ± 0.006
2B17	not detectable			0.21 ± 0.02	43.6 ± 9.3	0.005 ± 0.001

^a All data are the mean ± SD based on three independent experiments.

^b Homogenates from cells overexpressing UGTs 1A6, 2B4, 2B10 or 2B11 exhibited no detectable glucuronidating activity against endoxifen.

^c Low activity describes that fact that although some glucuronidation activity was observed for that UGT against a particular TAM metabolite, the level of detection was below sensitivity for kinetic studies.

Figure 1

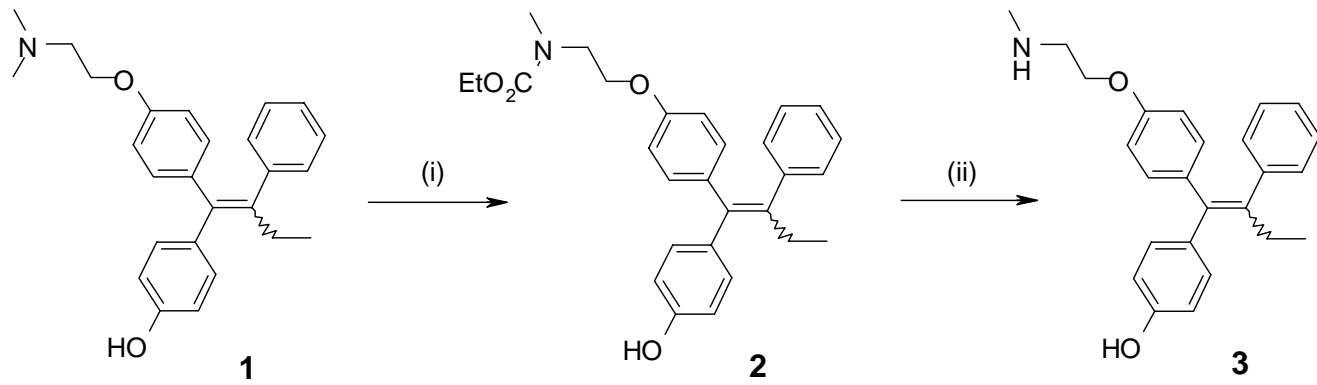


Figure 2

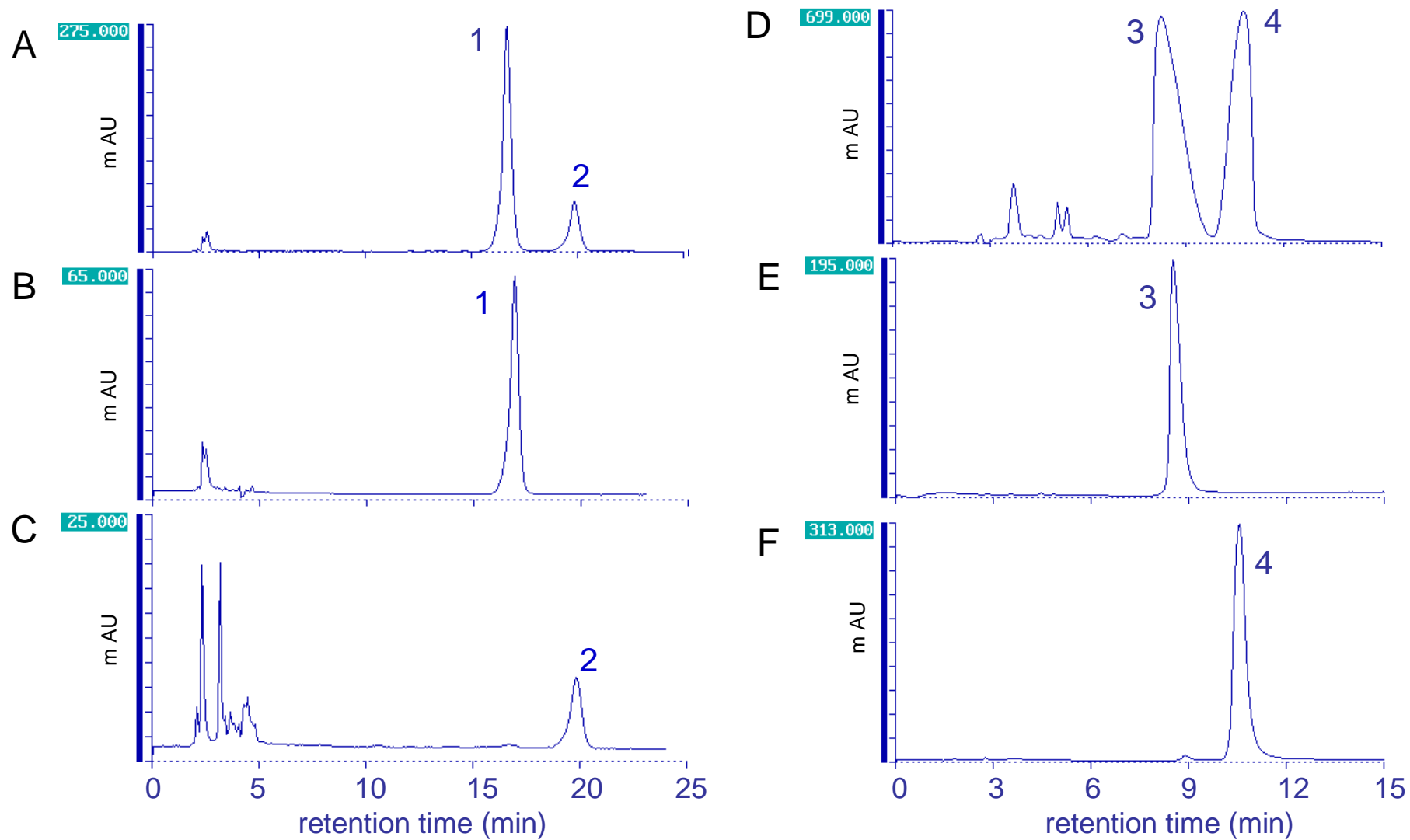


Figure 3

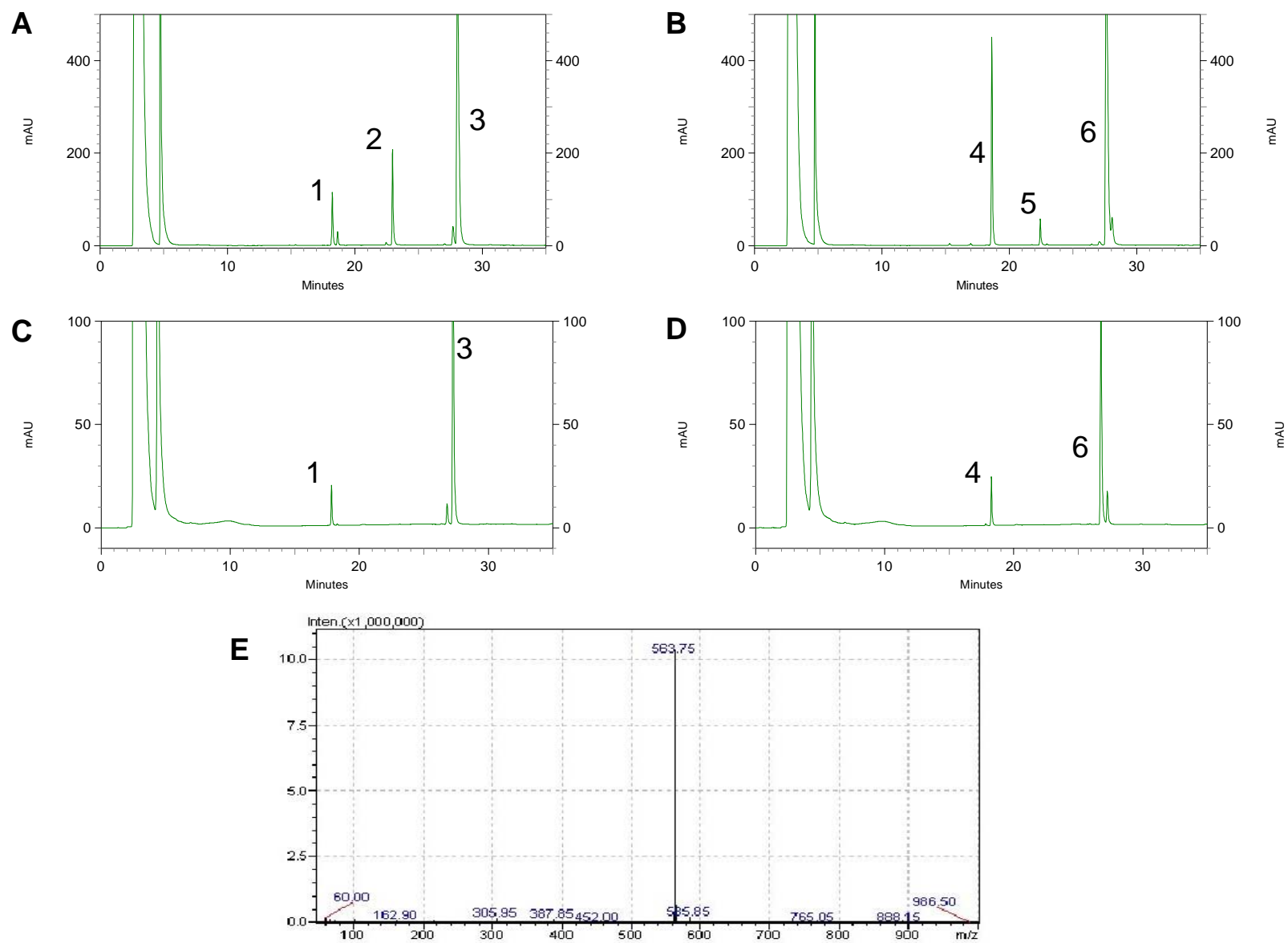
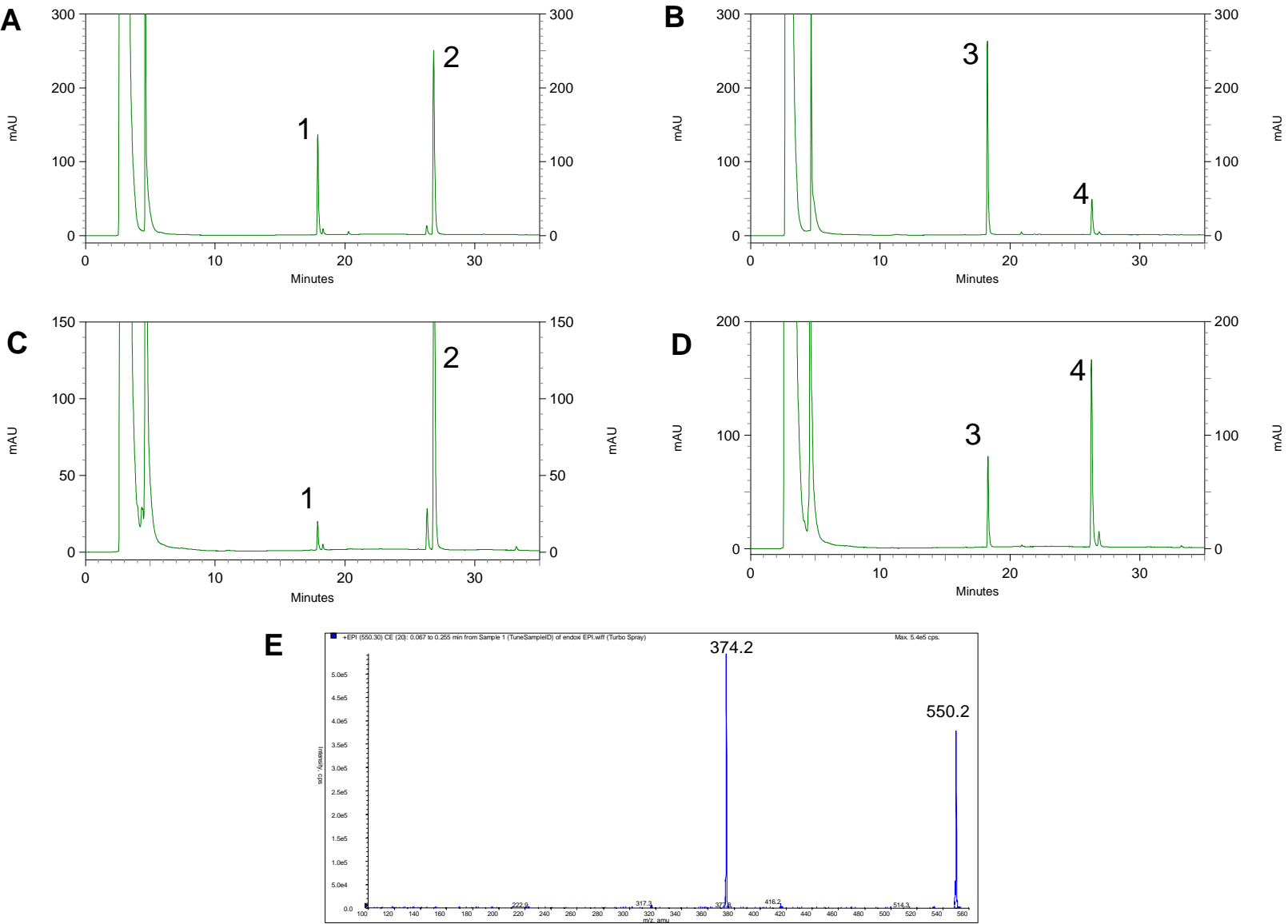


Figure 4



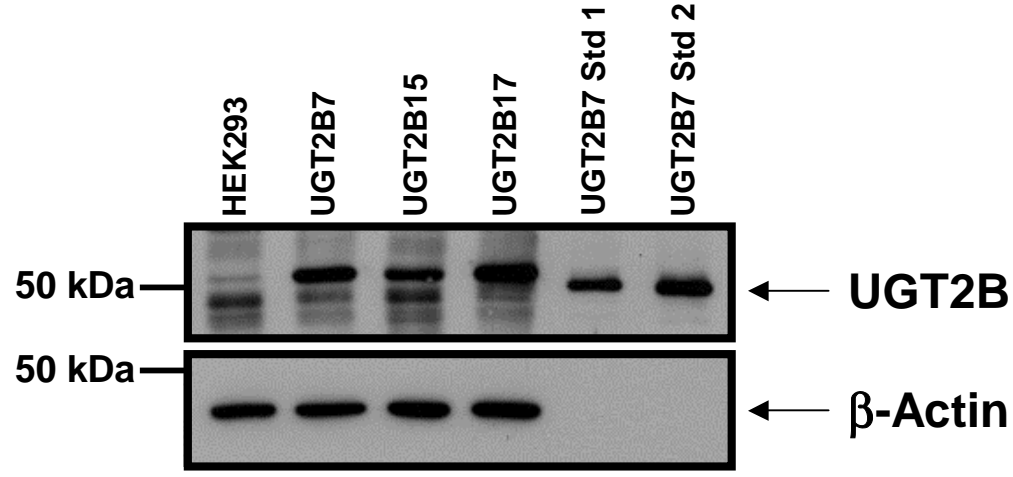


Figure 5